# Toroidal Circular and Elliptic Multipole Expansions within the Gap of Curved Accelerator Magnets

Pierre Schnizer*, Bernhard Schnizer†, Pavel Akishin‡, and Egbert Fischer*

*GSI Helmholtzzentrum für Schwerionenforschung GmbH, Planckstrasse 1, D-64291 Darmstadt, Germany
† Institut für Theoretische Physik-Computational Physics TU Graz, Petersgasse 16, A-8010 Graz, Austria
‡ Joint Institue for Nuclear Research LIT, Joliot-Curie 6, Dubna, Moscow Region, 141980, Russia
E-mail: p.schnizer@gsi.de

***Abstract*—Plane circular, toriodal circular and elliptic multipole expansions are used to reconstruct the magnetic field in the gap of accelerator magnets. Toroidal elliptic multipoles are obtained by approximate solution of the potential equation in a newly developed orthogonal coordinate system, the local toroidal elliptic coordinates.**
**Rotating coil probes are commonly used to measure the magnetic field of accelerator magnets. The artifacts, due to the geometry mismatch, are described for the toriodal circular multipoles.**

***Index Terms*—Magnetic field reconstruction, Toroidal circular and elliptic multipole expansions, Toroidal elliptic coordinates**

## I. Introduction

Present-day accelerator projects, as e.g. FAIR (Facilty for Antiproton and Ion Research) at GSI, strive to obtain higher energy resolution. This requires higher precision in the design and construction of the guiding and focusing magnets. So improvements of the computation, analytic representation and measurements of the field are needed. The usual method is to represent the plane central gap field a magnet by an expansion w.r.t. circular multipoles [1].

Curved magnets are typically measured with a long curved search coil [2]; this method only checks the magnet in its horizontal mid plane and not within the full aperture (see also Fig. 1). Rotating coils are typically used to obtain a harmonic field description within the a typically circular aperture (e.g. [3]) of a straight magnet. This method was extended to elliptic apertures [4] and is used to describe the field within magnets [5], [6]. The magnets of nearly all accelerators are curved (e.g. SIS100/SIS300 at GSI [7], NIKA in Dubna [8]).

The effects of the curvature of a magnet can be described by toroidal multipoles. These are approximate regular particular solutions of the potential equation in local circular or elliptic toroidal coordinates obtained by an expansion in the inverse aspect ratio of the torus. Circular coordinates are well known in the treatment of curved waveguides. The elliptic toroidal coordinates are really new.

## II. Multipole expansions

The plane irrotational source-free field in the gap and its potential are represented by various multipole expansions. Multipoles are a complete subset of particular solutions of the potential equations.

### A. Circular multipoles

The circular multipole expansion in polar coordinates $r, \theta$ is [1]:

$$\Phi(r,\theta) = \sum_{m=-\infty}^{\infty} C_m \; r^{|m|} \; e^{im\theta} \tag{1}$$

The coefficients $\mathbf{C}_m$ may be determined from a Fourier expansion of the field given along the reference circle $r = R_R$.

### B. Local circular toroidal coordinates

Such multipoles are regular particular solutions of the potential equation in dimensionless local toroidal coordinates $\rho, \vartheta, \varphi$, [9]. These are expressed in Cartesian coordinates $X, Y, Z$, whose centre coincides with that of the torus. $X$ and $Y$ lie in the equatorial plane. So the transformations are:

$$X + iY = R_C \; h \; e^{i\varphi}, \tag{2}$$
$$Z = R_{Ref} \; \sin\vartheta, \tag{3}$$
$$h = 1 + \epsilon \; \rho \; \cos\vartheta; \tag{4}$$
$$\epsilon = R_{Ref}/R_C. \tag{5}$$

$R_C$ is major radius = radius if curvature; $R_{Ref}$ minor radius = reference radius; $\epsilon$ the inverse aspect ratio.

*1) Multipole solutions:* Approximate (to the first order in $\epsilon$) torodoidally uniform particular solutions of the potential equation are obtained by approximate R-separation: $\Phi_m = h^{-1/2} \; \rho^m \; e^{im\vartheta}, \; m = 0, 1, 2, ...$ [10]. Introducing Cartesian coordinates $x, y$ in the plane $\varphi =$ const.:

$$\mathbf{z} = x + iy = R_{Ref} \; \rho \; e^{i\vartheta} \tag{6}$$

we get the approximate scalar toroidal multipoles:

$$\Phi_m(x,y) = \Big(\frac{\mathbf{z}}{R_{Ref}}\Big)^m - \frac{\epsilon}{4}\left[\Big(\frac{\mathbf{z}}{R_{Ref}}\Big)^{m+1} + \Big(\frac{\mathbf{z}}{R_{Ref}}\Big)^{m-1} \frac{|\mathbf{z}|^2}{R_{Ref}^2}\right]. \tag{7}$$

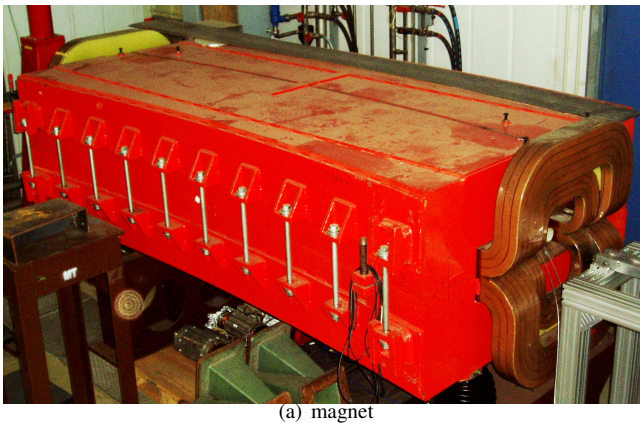

(a) magnet

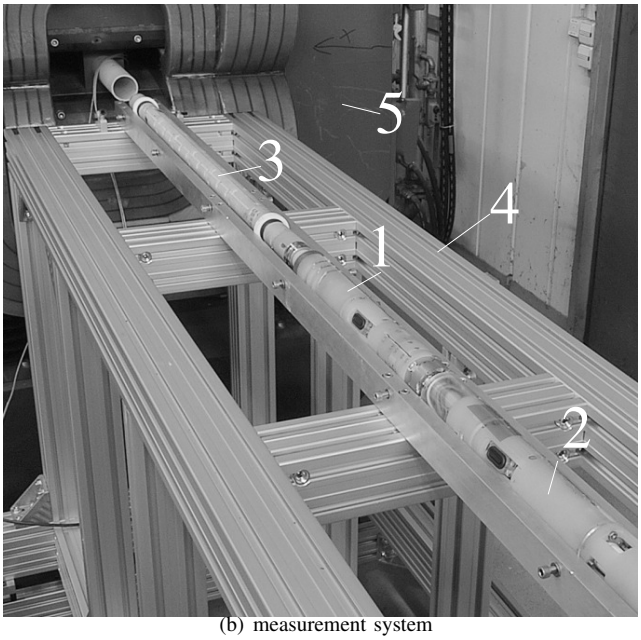


(b) measurement system

Fig. 1. A curved main dipole of the SIS18 and the mole in front of the magnet. The mole on the bench in front of a SIS18 magnet which was used for testing the mole. 1 ... motor unit 2 ... auxiliary unit 3 ... coil probe, 4 ... bench, 5 ... magnet

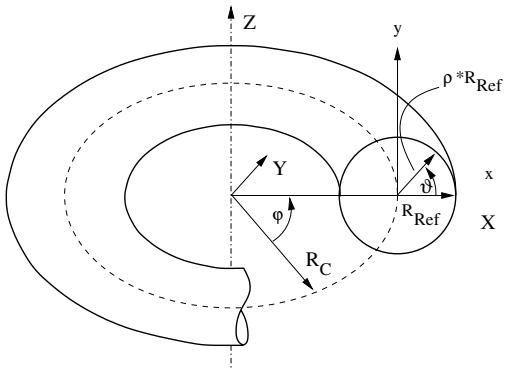


Fig. 2. The local toroidal coordinates

Corresponding (normal and skew) vector fields are:

$$\vec{T}_m(x,y) = -\frac{R_{Ref}}{m}\,\nabla\Phi_m(x,y), \tag{8}$$

$$\vec{T}_m^{(n)}(x,y) = \mathrm{Re}\left(\vec{T}_m(x,y)\right), \tag{9}$$

$$\vec{T}_m^{(s)}(x,y) = \mathrm{Im}\left(\vec{T}_m(x,y)\right). \tag{10}$$

A toroidally uniform magnetic induction may be represented as:

$$\vec{B}(x,y) = \sum_{m=1}^{M}\left(\bar{r}_m\,\vec{T}_m^{(n)}(x,y) + \bar{s}_m\,\vec{T}_m^{(s)}(x,y)\right). \tag{11}$$

### C. Elliptic Toroidal Multipoles

*1) Local Elliptic Toroidal Coordinates:* A plane elliptic system with coordinates $\bar{\eta},\bar{\psi}$ and excentricity $\bar{e}$ is shifted by the radius of curvature $R_C$ along the major axis. This system is then rotated around an axis parallel to the minor axis passing through the original position of the origin by the angle $\phi$. So we get the following orthogonal system:

$$X = \left(R_C + \bar{e}\,\cosh\bar{\eta}\,\cos\bar{\psi}\right)\cos\phi, \tag{12}$$

$$Y = \left(R_C + \bar{e}\,\cosh\bar{\eta}\,\cos\bar{\psi}\right)\sin\phi, \tag{13}$$

$$Z = \bar{e}\,\sinh\bar{\eta}\,\sin\bar{\psi}. \tag{14}$$

with the metric coefficients:

$$h_t = h_{\bar{\eta}} = h_{\bar{\psi}} = \bar{e}\sqrt{\cosh(2\bar{\eta})-\cos(2\bar{\psi})}/\sqrt{2}, \tag{15}$$

$$h_\phi = R_C + \bar{e}\,\cosh\bar{\eta}\cos\bar{\psi} \tag{16}$$

$$= R_C\,(1+\bar{\epsilon}\,\cosh\bar{\eta}\,\cos\bar{\psi}) = R_C\,\bar{h} \tag{17}$$

and the inverse aspect ratio

$$\bar{\epsilon} := \bar{e}/R_C. \tag{18}$$

Up to unessential constants the volume element is:

$$dV = \left(\cosh(2\bar{\eta})-\cos(2\bar{\psi})\right)\bar{h}d\bar{\eta}\,d\bar{\psi}\,d\phi \tag{19}$$

$$\sim h_{\bar{\eta}}\,h_{\bar{\psi}}\,h_\phi\,d\bar{\eta}\,d\bar{\psi}\,d\phi. \tag{20}$$

A segment of a torus with elliptic cross section is given by :

$$0 \le \bar{\eta} \le \bar{\eta}_0, \qquad -\pi \le \bar{\psi} \le \pi, \qquad -\phi_0 \le \phi \le \phi_0. \tag{21}$$

The excentricity is $\bar{e} = \sqrt{a^2-b^2}$, where $a,b$ are the major, minor axes of the ellipse bounding the cross section of the reference volume. $\tanh\bar{\eta}_0 = b/a$.

*2) The potential equation:* Up to some unessential constants the potential equation for toroidally (azimuthally) uniform potentials is:

$$\frac{1}{\cosh(2\bar{\eta})-\cos(2\bar{\psi})}\times \times\left[\frac{\partial^2}{\partial\bar{\eta}^2}+\frac{\partial^2}{\partial\bar{\psi}^2}-\frac{\bar{\epsilon}}{\bar{h}}\left(\sinh\bar{\eta}\cos\bar{\psi}\frac{\partial}{\partial\bar{\eta}}+\cosh\bar{\eta}\sin\bar{\psi}\frac{\partial}{\partial\bar{\eta}}\right)\right]\bar{\Phi} = 0. \tag{22}$$

The first fraction is removed and in the remaining part the dependent variable is changed from $\bar{\Phi}$ to $\sqrt{\bar{h}}\bar{\Phi}$ :

$$\frac{1}{\sqrt{\bar{h}}}\left[\frac{\partial^2}{\partial\bar{\eta}^2}+\frac{\partial^2}{\partial\bar{\psi}^2}-\frac{\bar{\epsilon}^2}{8\bar{h}^2}\left(\cosh(2\bar{\eta})-\cos(2\bar{\psi})\right)\right]\left(\sqrt{\bar{h}}\bar{\Phi}\right) = 0. \tag{23}$$

### D. Elliptic Toroidal Multipoles

If approximate solutions accurate to the first order in $\bar{\epsilon}$ are sufficient one may drop the last term in the square bracket of the preceding equation. The remaining two terms are just proportional to the potential equation in plane elliptic coordinates $\bar{\eta}, \bar{\psi}$. The complete set of particular solutions of the truncated equation has been given in [10], [4]. It comprises the functions:

$$\begin{array}{l} ce_0 = 1 \\ ce_n(\bar{\eta},\bar{\psi}) = \cosh(n\ \bar{\eta})\cos(n\bar{\psi}) \\ se_n(\bar{\eta},\bar{\psi}) = \sinh(n\ \bar{\eta})\ \ \sin(n\ \bar{\psi}) \end{array} \qquad n = 1,2,3,\ldots \tag{24}$$

So the corresponding approximate solutions of eq.(22) are:

$$\begin{aligned} \bar{\Phi}_{cn}(\bar{\eta},\bar{\psi}) &= (\bar{h})^{-1/2} ce_n(\bar{\eta},\bar{\psi}) + O(\bar{\epsilon}^2), && (25)\\ &= \mathcal{S}(\bar{\eta},\bar{\psi})\cosh(n\bar{\eta})\cos(n\bar{\psi}) + O(\bar{\epsilon}^2), && (26)\\ \bar{\Phi}_{sn}(\bar{\eta},\bar{\psi}) &= (\bar{h})^{-1/2} se_n(\bar{\eta},\bar{\psi}) + O(\bar{\epsilon}^2), && (27)\\ &= \mathcal{S}(\bar{\eta},\bar{\psi})\sinh(n\bar{\eta})\sin(n\bar{\psi}) + O(\bar{\epsilon}^2). && (28) \end{aligned}$$

with

$$\mathcal{S}(\bar{\eta},\bar{\psi}) = \left(1 + \bar{\epsilon}\frac{1}{2}\cosh(n\bar{\eta})\cos(n\bar{\psi})\right) \tag{29}$$

Other expressions may be obtained by use of trigonometric and hyperbolic addition theorems. All these elliptic toroidal multipoles are mutually orthogonal under:

$$\int_0^{2\pi} \Phi_{\alpha,n}\ \Phi_{\beta,n'}\ \bar{h}\ d\bar{\psi} \tag{30}$$

### E. Elliptic Toroidal Vector Fields

Such vector fields are obtained from the multipoles just given by gradients:

$$\begin{aligned} \vec{F}_{cn} &= -\frac{1}{h_t}\left(\frac{\partial}{\partial\bar{\eta}}, \frac{\partial}{\partial\bar{\psi}}\right)\bar{\Phi}_{cn}, && (31)\\ \vec{F}_{sn} &= -\frac{1}{h_t}\left(\frac{\partial}{\partial\bar{\eta}}, \frac{\partial}{\partial\bar{\psi}}\right)\bar{\Phi}_{sn}. && (32) \end{aligned}$$

The working of these toroidal multipoles and vector fields is under further investigation.

## III. Application: Reproducing theoretical fields

Two-dimensional field values for long curved dipole magnets were computed by a numerical program. The values belonging to a plane $\varphi =$ const. were interpolated and integrated to give a potential. The latter was expanded w.r.t. the toroidal multipoles (7) and also w.r.t. the common circular multipoles $(r/R_{Ref})^m\ e^{im\theta}$. Both approaches give good representations. The expansion coefficients differ since in the former expansion the effect of the curvature is contained in the basis functions while in the latter expansion this effect is hidden in the expansion coefficients.

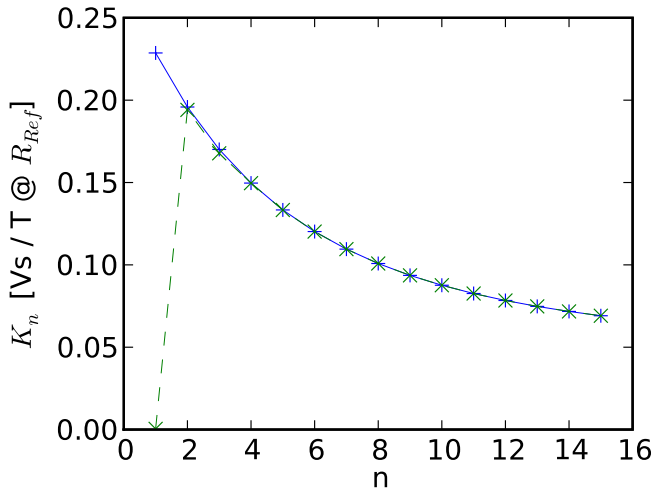


Fig. 3. The coil sensitivity $K_n$ versus the multipole $n$ (absolute…'+', compensated …'-')

## IV. Application: Rotating coil in a curved magnet

### A. Excursus: Rotating coil in a straight magnet

The output of a radial coil rotating with constant angular frequency $\omega$ in a magnetic field is Fourier decomposed as:

$$V(t) = -\omega\sum_{n=1}^{M} K_n\left(a_n\ \cos(n\omega t)\ +\ b_n\ \sin(n\omega t)\right), \tag{33}$$

with $a_n$, $b_n$ the multipole components of the magnetic field. The upper limit of the sum, $M$ can be $\infty$. In practice a value between 10 and 20 is used. The sensitivity of a so called radial coil probe to the multipole n is given by

$$K_n = \frac{NLR_{Ref}}{n}\left[\left(\frac{r_2}{R_{Ref}}\right)^n - \left(\frac{r_1}{R_{Ref}}\right)^n\right]. \tag{34}$$

with L the length of the coil, $r_2$ and $r_1$ the other and inner radius of the coil [3], [11] and $R_{Ref}$ the reference radius. The factors are given for one coil array as used at CERN [11], [12] (see Fig. 3, absolute curve). During the measurement the axis of the coil probe does not necessarily coincide with the magnet's axis, but has an offset $d$. This is taken into account correcting the multipoles $a_n$ and $b_n$ applying the "feed down"

$$a_n = \sum_{m=n}^{M}\binom{n-1}{n-m}\left(\frac{d}{R_{Ref}}\right)^{n-m} a'_m\,. \tag{35}$$

The same procedure is applied for converting $b'_n$ to $b_n$.

### B. Induced voltage

The coil's rotation axis is in the equatorial plane of the torus segment, which is the reference volume in the gap of the curved magnet. $d$ is its distance from the central circle; $d$ is located at $\varphi = 0$. $L = \ell$ is the coil length. $r_1$ and $r_2$ are the distances of the big parts of the coil from the rotation axis.

The rotating coil excises a circular cylinder within the toroidal segment. By assumption, the field is the same in each cross section $\varphi =$ const. and is given by (11). At the contrary, the field is a really three-dimensional one across the cylinder.

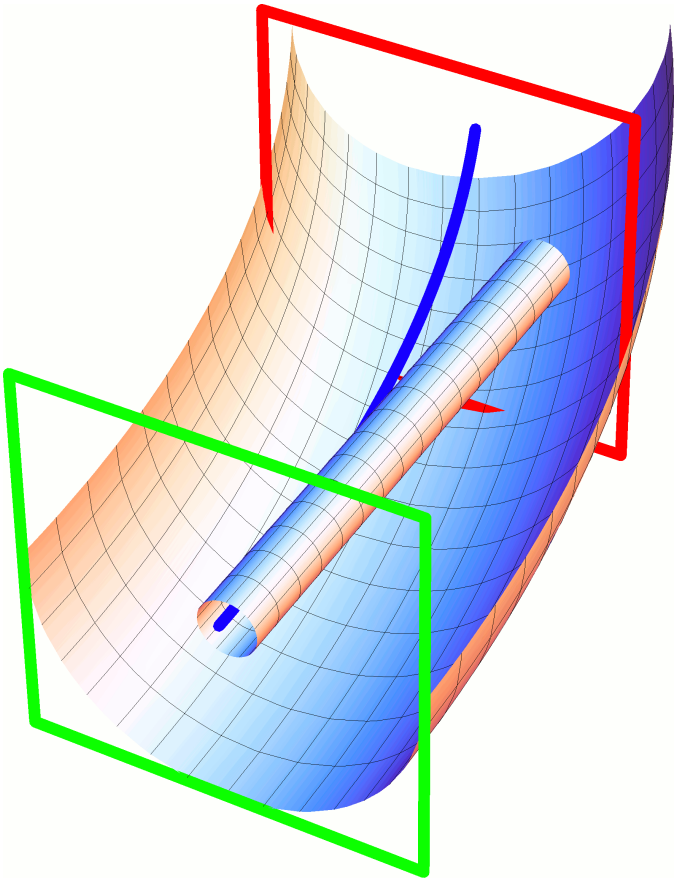

Fig. 4. The rotating coil probe within the curved magnet aperture.

A Cartesian $(x, y, z)$ and a cylindrical $(r, \theta, z)$ system are introduced. Their equatorial planes are at $\varphi = 0; y = Z, Y = -z$. So each point of the coil may be denoted by each of the triples $(x, y, \varphi)$ and $(r, \theta, z)$. The transformations between these triples have been derived in [10].

The Voltage induced in the rotating coil is according to Faraday's law:

$$V(t) \;=\; -\frac{d\Phi}{dt} \;=\; -\,\frac{d}{dt}\int_{r_1}^{r2}\int_{-L}^{L}(\vec{B}\cdot\vec{e}_r)\;dz\;dr. \qquad (36)$$

Expression (11) is used for $\vec{B}$ above but the transformations to be applied for the components and arguments are derived in eqs.(44) to (49) of [10]. We evaluated the integrands by *Mathematica* and found:

$$V(t) = \omega\sum_{m=1}^{M} K_n\left[\bar{s}_m\; C_{mn}\cos(n\omega t) - \bar{r}_m D_{mn}\sin(n\omega t)\right] \qquad (37)$$

Equating (33) to (37) and comparing the coefficients of equal harmonics gives:

$$a_n = -\sum_{m=1}^{M}\bar{s}_m\; C_{mn}, \qquad b_n = \sum_{m=1}^{M}\bar{r}_m\; D_{mn}. \qquad (38)$$

Multiplying the above equations by the inverse (or pseudoinverse) matrices $C^{-1}$, $D^{-1}$ respectively, gives the wanted expansion coefficients

$$\bar{s}_k \;=\; -\sum_{n=1}^{M(+1)} a_n\; D^{-1}_{nk}, \qquad \bar{r}_k \;=\; \sum_{n=1}^{M(+1)} b_n\; C^{-1}_{nk}. \qquad (39)$$

The elements of the matrices $(C_{nm})$ and $(D_{nm})$ are given below. The evaluations of $(C_{nm})$ and $(D_{nm})$ reveal that the matrices $C$ and $D$ are nealy the same. Their difference $dC$ is a matrix, whose only non-zero elements are in the first column. Their values are :

$$(dC)_{m,1} = \;-\;\epsilon\left(\frac{d}{2R_{Ref}}\right)^m. \qquad (40)$$

So it suffices to compute only one matrix, say $C$. $D$ then follows from:

$$D = C + dC. \qquad (41)$$

Each matrix element of $C$ and $D$ comprises at most 4 terms. The conversion matrix $(C_{nm})$ can be written in the following form

$$C = I - \epsilon\big(U + \underbrace{\mathcal{D} + \mathcal{L}^{co} + \mathcal{L}^{dr2}}_{f(d)}\big) + \mathcal{L}^{dr}. \qquad (42)$$

The matrix consists of four submatrices whose magnitude depend on the ratio $\epsilon = R_{Ref}/R_C$. Only the first matrix U is independent of the coil probes offset from the coordinate system. All matrices dependent on d are zero if $d = 0$. $U$ is given by

$$U = \frac{n}{4(m-1)}\;\delta_{n+1,m} \qquad (43)$$

and $D$ by

$$\mathcal{D} = \frac{d}{4R_{Ref}}\;\delta_{nm}\cdot\begin{cases} 2 & n = 1 \\ n+2 & n > 2 \end{cases}. \qquad (44)$$

All following matrices (denoted with a large $\mathcal{L}$) are lower triangular matrices with all elements on the diagonal equal to zero, thus $\mathcal{L}$ is given by

$$\mathcal{L} = \lambda_{nm} = \begin{cases} 0 & n \le m \\ \neq 0 & n > m \end{cases}. \qquad (45)$$

The matrix $\mathcal{L}^{co}$ is given by

$$\mathcal{L}^{co} = \binom{n-2}{n-m-1}(n-1)\left(\frac{d}{R_{Ref}}\right)^{n-m-1} S^c \qquad (46)$$

with $S^c$ given by

$$S^c = \Big[\underbrace{\frac{l^2}{24R^2_{Ref}}}_{S^{cl}} - \frac{K_{m+2}}{4\,(m+1)\,K_m}\Big]. \qquad (47)$$

$S^m$ describes the smear out of one toroidal multipole on the whole spectrum measured by the rotating coil depending on the curvature of the torus (described by $\epsilon$ and the coil geometry).

The matrix $\mathcal{L}^{dr2}$ is given by

$$\mathcal{L}^{dr2} = \frac{4}{n-m+1}\left(\frac{d}{R_{Ref}}\right)^{(n-m+1)} * C^{dr2} \qquad (48)$$

TABLE I
PARAMETERS FOR DIFFERENT MACHINES.

| | $R_C$ [m] | $R_{Ref}$ [mm] | $\epsilon$ [units] | $L$ [mm] | d [mm] |
|---|---|---|---|---|---|
| LHC | 4650 | 17 | 0.04 | 600 | 1 |
| SIS100 | 52.5 | 40 | 7.62 | 600 | 1 |
| SIS300 | 52.5 | 35 | 6.67 | 600 | 1 |
| NICA | 15 | 40 | 26.67 | 600 | 1 |

with $C^{dr2}$

$$C^{dr2} = \begin{pmatrix} 0 & 0 & 0 & 0 & 0 & 0 & 0 & 0 & 0\ 0\ 0 \\ 4 & 0 & 0 & 0 & 0 & 0 & 0 & 0 & 0\ 0\ 0 \\ 6 & 12 & 0 & 0 & 0 & 0 & 0 & 0 & 0\ 0\ 0 \\ 8 & 24 & 21 & 0 & 0 & 0 & 0 & 0 & 0\ 0\ 0 \\ 10 & 40 & 54 & 32 & 0 & 0 & 0 & 0 & 0\ 0\ 0 \\ 12 & 60 & 110 & 100 & 45 & 0 & 0 & 0 & 0\ 0\ 0 \\ 14 & 84 & 195 & 240 & 165 & 60 & 0 & 0 & 0\ 0\ 0 \\ 16 & 112 & 315 & 490 & 455 & 252 & 77 & 0 & 0\ 0\ 0 \\ 18 & 144 & 476 & 896 & 1050 & 784 & 364 & 96 & 0\ 0\ 0 \\ 20 & 180 & 684 & 1512 & 2142 & 2016 & 1260 & 504 & 117\ 0\ 0 \end{pmatrix}.$$

The star "*" indicates that the multiplication has to be done element by element. A short formula is not yet available for $C^{dr2}$.

The matrix $\mathcal{L}^{dr}$ is the only one, which does not depend on the torus curvature ratio $\epsilon$. Its non zero elements are given by

$$\mathcal{L}^{dr} = \binom{n-1}{n-m} \left(\frac{d}{R_{Ref}}\right)^{n-m} . \quad (49)$$

This term is equivalent to the formula derived for recalculating plane circular multipoles This term is the equivalent as found, when a coil probe is translated by a distance $d$ in a cylindrical field [1].

For the discussion below the matrix $M_{co}$ is defined

$$M^{co}_{nm} = \binom{n-2}{n-m-1} (n-1) \frac{l^2}{24 R^2_{Ref}} \left(\frac{d}{R_{Ref}}\right)^{n-m-1} . \quad (50)$$

It is obtained from $L^{dr}$ only using $S^{cl}$, setting the second term of $S^m$ to zero.

The matrices $C$ and $D$ can be inverted numerically.

### C. Magnitude of the terms

The formulae given above were evaluated for the following different machines: the Large Hadron Collider (LHC) at CERN [13], SIS100 [6], [7] and SIS300 at GSI, and NICA [8] at Dubna (see Table I).

The parameters given in Table I were used to calculate the coefficients of the matrices. Accelerators require a field description with an accuracy of $1unit$ and roughly $0.1$ unit for the field homogeneity (1 unit equals 100 ppm). Therefore any contribution less than 1 ppm can be ignored.

Due to the circumference of the LHC $\epsilon$ is very small and thus the correction of all matrices are very small (less than 1 ppm) except for the matrix $M_{co}$, where the values close to the diagonal get to a size of 2000 ppm. This value may seem to exceed the target value for the field description; but the higher order multipoles are in the order of 100 ppm; thus the effective artifact will be safely below the target value of 10 ppm.

For machines with an aspect ratio as found for SIS100 or SIS300 the matrix $U$ is in the order of 100 ppm. It can be neglected except for the main multipole. The values of the matrix $M_{co}$ get of similar size as the values for $L_{dr}$. The values are given by the offset d. Also when measuring straight magnets special methods are applied to obtain the offset d from the measured dataset [3]. Thus the authors believe that the artifacts can be minimised by similar adequate procedures [14].

### D. Choosing the coil length

A long coil will result in larger sensitivity (see (34)) and thus in better measurement performance. On the other hand the matrix $L_{co}$ depends on the coil length (see (47)). The magnitude of the coefficients depends on $d$ as for to $L_{dr}$, with the component $S_{ml}$ being orders of magnitude larger than the second term of $S_m$. So the dominating part of $L_{co}$ can be written as

$$M_{co} = \binom{n-2}{n-m-1} (n-1) \frac{l^2}{24 R^2_{Ref}} \left(\frac{d}{R_{Ref}}\right)^{n-m-1} . \quad (51)$$

Its total contribution to the matrix $C_{nm}$ is given by $\epsilon M_{co}$.

$$\epsilon M_{co} = \frac{l^2 \epsilon}{24 R_{Ref} d} (n-m) L_{dr} \quad (52)$$

The factor (n - m) varies across the matrix; practically not more than 15 coefficients will be used. Therefore the coil length should be in the range of

$$l = \sqrt{\frac{24\, d}{\epsilon\, R_C}} . \quad (53)$$

### E. Compensating systems

The main multipole of an accelerator magnet is typically 1000 to 10000 times larger than the higher order multipoles. Therefore one reduces the sensitivity to the main component subtracting two coil rotating on a common support (e.g. [3], [11]). $K_1$ is typically reduced by a factor 500 to 1000 for a carefully fabricated coil array. This setup increases the measurement accuracy of the higher order multipoles, as the coil probe system is more immune to mechanical imperfections of the rotation, and less accurate electronics are required. The compensated factors $K_n$ is illustrated in Fig. 3.

The second term of (47) contains the ratio $K_{n+2}/K_n$, which would get large. The multipole $C_1$, measured with the compensated system is not used in the field calculation, but it is taken from the measurement with the "absolute coil probe". Therefore $K_1$ of the absolute system is to be used in the ratio.

### F. Comparison to a simplistic approach

A common approach describing the field of curved magnets is using two dimensional circular multipoles, neglecting any dependence in z. The local toroidal multipoles, given above, allow estimating the error artefacts created by this approach.

The sagitta of a beam in a dipole magnet can be approximated by

$$s \approx \frac{l^2_{dp}}{8\ R_{Ring}} \quad (54)$$

(a) to scale (b) radius reduced

Fig. 5. Overlap of the coils

with $s$ the sagitta, $l_{dp}$ the length of the chord and $R_{Ring}$ the radius of the ring. The sagitta for the SIS100 magnet is given by

$$s \approx \frac{(3[m])^2}{8 \cdot 52.5[m]} \approx 23[mm] \tag{55}$$

and the sagitta within the coil (length $L$ 600 mm) is

$$s \approx \frac{(0.6[m])^2}{8 \cdot 52.5[m]} \approx 0.9[mm] \tag{56}$$

Straight magnets are measured, placing the rotating coil sequentially along the magnet bore. The same approach, applied in a curved magnet will lead to a overlap one side and a gap on the other see (Fig. 5) [15]. The overlap length is given by

$$d_U = \frac{LR}{R_{Ring}} \tag{57}$$

with $d_U$ the overlap length, $R$ the coil radius (typically close to $R_{Ref}$). This simplified approach results in an relative error independent of the coil length

$$\frac{d_U}{L} = \frac{D}{2\,R_{Ring}} = \frac{80 \cdot 10^{-3}}{2 \cdot 12.5} = 32 \cdot 10^{-4}\,. \tag{58}$$

The overlap results, that a part on the outside is not covered, while some part at the inner side is taken twice. Thus only the harmonics $(-1)^{(n-1)} \cdot z^{(n-1)}$ are affect, these terms are the non allowed ones in a dipole. Further this ratio is too small to be significant for any of the machines listed in Table I.

The results of the toroidal multipoles and this plane circular multipoles can only be compared on the field description. This simplified calculation does not consider an offset d from the axis. So only the term $U$ is nonzero in (42). The size of this parameter is proportional $\epsilon$. The inverse matrix of

$$(I - \epsilon U)^{-1} = I + \epsilon U + O(\epsilon^2)\,. \tag{59}$$

XXX to be checked!! Thus this term does not compensate the derivative of the first term in $\epsilon$ of (20), but differs by $1/(m-1)$. Thus this simple approach is only valid if this difference is negligible next to the other terms in (20).

## V. Conclusions

The field description of accelerator magnets was extended from the usually used circular multipoles to ones adapted to elliptic apertures [4], commonly used in most accelerators, as well as to curved magnets, typically found in medium sized accelerators.

Rotating coil probes allow measuring circular 2D harmonic coefficients. Using the circular toroidal multipoles the expected artifacts are described and a measure for an acceptable coil length is given.

## References


[1] A. K. Jain, "Basic theory of magnets," in *CAS Magnetic Measurement and Alignment*, S. Turner, Ed. CERN, August 1998, pp. 1–21.

[2] G. Moritz, "Mechanical equipment," in *CAS Measurement and Alignment of Acclerator and Detector Magnets*, S. Turner, Ed. CERN, April 1998, pp. 251–272.

[3] A. K. Jain, "Harmonic coils," in *CAS Magnetic Measurement and Alignment*, S. Turner, Ed. CERN, August 1998, pp. 175–217.

[4] P. Schnizer, B. Schnizer, P. Akishin, and E. Fischer, "Theory and application of plane elliptic multipoles for static magnetic fields," *Nuclear Instruments and Methods in Physics Research Section A: Accelerators, Spectrometers, Detectors and Associated Equipment*, vol. 607, no. 3, pp. 505 – 516, 2009. [Online]. Available: http://www.sciencedirect.com/science/article/B6TJM-4WH8C2J-4/2/7f3973c2a3a41e616d9ec8901a2f3a9d

[5] E. Fischer, P. Schnizer, P. Akishin, R. Kurnyshov, A. Mierau, B. Schnizer, and P. Shcherbakov, "Measured and calculated field properties of the SIS100 magnets described using elliptic and toroidal multipoles," in *PAC 09, Vancouver 2009*, 2009.

[6] E. Fischer, P. Schnizer, A. Akishin, R. Kurnyshov, A. Mierau, B. Schnizer, S. Y. Shim, and P. Sherbakov, "Superconducting SIS100 prototype magnets design, test results and final design issues," *IEEE T. Appl. Supercon.*, vol. 20, no. 3, pp. 164–167, June 2010.

[7] "FAIR - Facility for Antiprotons and Ion Research, Technical Design Report, Synchrotron SIS100," December 2008.

[8] H. G. Khodzhibagiyan *et al.*, "Superconducting magnets for the nica accelerator complex in dubna," this conference.

[9] W. D. D'haeseleer, W. N. G. Hitchon, J. D. Callen, and J.-L. Shohet, *Flux coordinates and magnetic field structure*. Springer, 1990.

[10] P. Schnizer, B. Schnizer, P. Akishin, and E. Fischer, "Plane elliptic or toroidal multipole expansions for static fields. applications within the gap of straight and curved accelerator magnets," *The International Journal for Computation and Mathematics in Electrical Engineering (COMPEL)*, vol. 28, no. 4, 2009.

[11] P. Schnizer, "Measuring system qualification for LHC arc quadrupole magnets," Ph.D. dissertation, TU Graz, 2002.

[12] N. Smirnov, L. Bottura, F. Chiusano, O. Dunkel, P. Legrand, S. Schloss, P. Schnizer, and P. Sievers, "A system for series magnetic measurements of the lhc main quadrupoles," *IEEE T. on Applied Superconductivity*, vol. 12, no. 1, pp. 1688 – 1691, March 2002.

[13] O. Brüning, P. Collier, P. Lebrun, S. Myers, R. Ostojic, J. Poole, and P. Proudlock, *LHC Design Report*. Geneva: CERN, 2004.

[14] L. Bottura, M. Buzio, G. Deferne, P. Schnizer, P. Sievers, and N. Smirnov, "Magnetic measurement of alignment of main lhc dipoles and associated correctors."

[15] P. Schnizer, "Vermessung von gekrümmten Supraleitenden Magneten," HESR Magnet Meeting @ GSI, March 2007.